Hindawi
Advances in Mathematical Physics
Volume 2023, Article ID 4132763, 16 pages
https://doi.org/10.1155/2023/4132763

Research Article

The Modulation Instability Analysis and Analytical Solutions of the Nonlinear Gross–Pitaevskii Model with Conformable Operator and Riemann Wave Equations via Recently Developed Scheme

Wei Gao [1] **and Haci Mehmet Baskonus** [2]

[1]*School of Information Science and Technology, Yunnan Normal University, Kunming, 650500, China*
[2]*Department of Mathematics and Science Education, Faculty of Education, Harran University, Sanliurfa, 63050, Türkiye*

Correspondence should be addressed to Haci Mehmet Baskonus; hmbaskonus@gmail.com

Received 25 December 2022; Revised 13 August 2023; Accepted 28 October 2023; Published 28 November 2023

Academic Editor: Ghulam Rasool

In this manuscript, we focus on the application of recently developed analytical scheme, namely, the rational sine-Gordon expansion method (SGEM). Some new exact solutions of Riemann wave system and the nonlinear Gross–Pitaevskii equation (GPE) by using this method are extracted. This method is based on the general properties of the SGEM which uses the fundamental properties of trigonometric functions. Many novel analytical solutions such as dark, bright, mixed dark–bright, hyperbolic, and periodic wave solutions are successfully extracted. Physical meanings of solutions are simulated by the various figures in 2D and 3D along with the contour graphs. Strain conditions of the existence are also reported in detail. Finally, modulation instability analysis of the nonlinear GPE is studied in detail.

1. Introduction

In modern century, the real-world problems arising in various fields of daily life, particularly, engineering such as computer viruses, cyber security, artificial intelligence, magnetism, physics, oceanography, and so on have been symbolized via mathematical norms. Scientists have investigated their connections among multidisciplinary properties. For the last several decades, newly developed mathematical properties have been used to explain many physical problems [1–5]. In [6], scientists have applied the Hopf Bifurcation theorem on the models arising in the group competitive martial arts. In [7], the modified double Laplace transform method is handled to extract some results of the pseudo-hyperbolic telegraph model. The relativistic wave equation associated with the Schrödinger equation was studied in terms of traveling wave distribution in [8]. Wazwaz [9, 10] introduced the several optical solitons for $(2+1)$-dimensional Schrödinger (NLS) equation. In [11], modified exponential function method have been applied to the nonlinear Gerdjikov–Ivanov equation with the M-fractional. Hu et al. [12] focused on the rational and semirational properties of B-type Kadomtsev Petviashvili Boussinesq model. Kudryashov [13] presented the Lax pair and the first integrals for some mathematical properties. Ghanbari et al. [14] observed the rational function solutions for the extended Zakharov Kuzetsov equation. M-type dark soliton facts in optical fibers have been investigated by Yao et al. [15]. Hybrid method has been applied into Rosenau–Hyman equation [16]. Real quadratic fields have been focused on the Handy method in [17]. Generalized $(3+1)$ Shallow Water-Like (SWL) equation was observed by Dusunceli [18]. The perturbed Schrödinger and the Heisenberg ferromagnetic spin chain have been investigated in [19, 20]. Park et al. [21] have observed the fifth-order Korteweg-de Vries equations. The multiple exp-function method has been applied on some mathematical models [22]. Chebyshev series have been used to investigate numerically the integro-differential equations in [23]. Duffing and diffusion reaction models have been investigated in the M-derivative operator in [24].

W-shape properties of the $(3+1)$-dimensional nonlinear evolution equations have been reported in [25]. The general and wide-spectral explicit properties of the complex coupled Maccari system have been introduced in [26]. The superconductivity models have been studied in [27]. The Benjamin–Bona–Mahony–Peregrine equation with power law nonlinearity has been studied in [28]. The finite element method have been used to observe a surface plasmon resonance (SPR) sensor in [29]. A current decoupling control strategy was considered on combining a fast terminal sliding mode control and an adaptive extended state observer [30]. A Robust Hammerstein–Wiener Model identification method was applied in [31]. A robust model predictive current control scheme was proposed in [32]. Liu and Liu [32] have studied on the photoacoustic microfluidic pumps [33]. A linear AC unit commitment formulation have been presented in [34]. Moreover, seismic-wave attenuation, shear-wave attenuations, and waves with a wide range of frequencies in digital core have been introduced [35–38]. Some control problems and optimization application have been presented [39–45]. In [46], bipolar cubic fuzzy graphs have been studied. The shallow ocean-waves and rogue waves with translational coordination have been observed in [47, 48]. The influence of Woods–Saxon potential was presented in [49]. Soliton, numerical, and closed solutions of nonlinear models have been investigated by using various schemes [49–56]. To represent the wave's amplitude, simplest equation algorithms have been used by Inc et al. [57]. Az-Zo'bi et al. [58] studied and used to observe the pulses propagation with power nonlinearity via conformable. Some novel liquid crystals models have been investigated by using some analytical schemes in [59]. Ur Rahman et al. [60] extracted the deeper properties of the fractional regularized long-wave Burgers problem by using two different fractional operators, Beta and M-truncated. In [61], the fractional Huxley equation with Beta and M-truncated derivatives have been considered for reporting nonlinear coherent structures arising in a variety of environments, like spectrum energy, applied mathematics, mechanics, control theory, biology, seismology, and many more.

One of such models belongs to the Riemann wave systems (RWS) defined by the following:

$$\begin{aligned} V_t+\ &\alpha\Psi_{xyy}+\beta\Psi V_y+\gamma U V_x=0,\\ &V_y=U_x,\\ &V_x=\Psi_y, \end{aligned} \tag{1}$$

being α, β, and γ are constants. RWS studied in this paper are used to explain the tidal and tsunami waves in ocean [62]. The nonlinear terms of first equation in Equation (1) give the stationary wave propagation properties in the frame of physical sense. Kundu et al. [63] investigated the parametric analysis via sine-Gordon expansion method (SGEM). Gurevich et al. [64] has used the slow modulation method. They have applied the generalized hodograph method to find some analytical solutions.

Another important model is considered as follows:

$$\begin{aligned} i\frac{\partial}{\partial t}\Psi(x,t)=&-\frac{\partial^2}{\partial x^2}\Psi(x,t)-\frac{1}{2}\lambda^2x^2\Psi(x,t)\\ &+2N\frac{a_s}{l_\perp}|\Psi(x,t)|^2\Psi(x,t), \end{aligned} \tag{2}$$

in which $\lambda \ll 1$, N is a constant value and a_s is the axial and transverse harmonic oscillator frequencies. This equation is used to describe the rogue wave in the evolution of the macroscopic wave function of Bose–Einstein condensates (BECs) and also to investigate the deeper properties at the mean-field level [65], via

$$\Psi(x,t)=q(X,T)e^{\lambda t/2-i\lambda x^2/4}, \tag{3}$$

in which equation $X=xe^{\lambda t}$, $T=2\int_0^t e^{2\lambda\tau}d\tau$, the nonlinear Gross−Pitaevskii equation (GPE) can be rewritten as follows [66, 67]:

$$i\frac{\partial^\theta q}{\partial T^\theta}+\frac{1}{2}\frac{\partial^2 q}{\partial X^2}-\Upsilon|q|^2q=0, \tag{4}$$

in which $q=q(X,T)$, $\Upsilon=\frac{Na_0}{l_\perp}$, θ is conformable derivative order in $0<\theta<1$. Equation (4) arises in the magnetic field theory observed by magnetically tuning the interatomic interaction.

The paper is organized as follows. In Section 2, the rational sine-Gordon expansion method (RSGEM) is given in detail. In Section 3, RSGEM is applied to extract the stationary optical solitons, mixed dark, and bright solitons to the Equations (1) and (4). Additionally, stability properties of the complex mixed dark–bright soliton solutions are also reported. Finally, the paper is completed by presenting the important novelties of this paper in Section 4.

2. General Properties of RSGEM

This part introduces the general properties of RSGEM, First, let us consider the following sine-Gordon equation [68–70].

$$u_{xx}(x,t)-u_{tt}(x,t)=m^2\sin(u(x,t)). \tag{5}$$

Here, m is a real constant with nonzero. Taking the traveling wave transformation as $u(x,t)=U(\xi)$, $\xi=\mu(x-ct)$ into Equation (5) produces

$$U''=\frac{m^2}{\mu^2(1-c^2)}\sin(U), \tag{6}$$

where $U=U(\xi)$, $U''=\frac{d^2U}{d\xi^2}$ and c, μ are also real constants with nonzero. With some calculations, it may be obtained as follows:

$$\left(\left(\frac{U}{2}\right)'\right)^2=\frac{m^2}{\mu^2(1-c^2)}\sin^2\left(\frac{U}{2}\right)+k, \tag{7}$$

where k is an integral constant. For simplicity, by considering as $k=0$, $\omega=\frac{U}{2}$, and $a^2=\frac{m^2}{\mu^2(1-c^2)}$, Equation (7) reads as follows:

$$w' = a\sin(w), \tag{8}$$

in which $w = w(\xi)$. Gaining $a = 1$ in Equation (8), we obtain the following two interesting and important relationship

$$\sin(w) = \sin[w(\xi)] = \frac{2pe^{\xi}}{p^2e^{2\xi}+1}\downarrow p_{=1} = \mathrm{sec}h(\xi), \tag{9}$$

$$\cos(w) = \cos[w(\xi)] = \frac{2pe^{\xi}}{p^2e^{2\xi}+1}\downarrow p_{=1} = \tan h(\xi). \tag{10}$$

Let us take into account the general mathematical model as follows:

$$P(\Psi, \Psi_x, \Psi_{xt}, \Psi^2, \cdots) = 0. \tag{11}$$

Taking into account as $\Psi = \Psi(x,t) = U(\xi)$, $\xi = \mu(x - ct)$, it is converted as follows:

$$N(U, U', U'', U^2, \cdots) = 0. \tag{12}$$

Here $U = U(\xi)$, $U' = \frac{dU}{d\xi}$. In Equation (12), the trial equation for solution function may be considered as follows:

$$U(\xi) = \frac{\sum_{i=1}^{n}\tan h^{i-1}(\xi)[A_i\,\mathrm{sec}h(\xi) + c_i\tan h(\xi)] + A_0}{\sum_{i=1}^{m}\tan h^{i-1}(\xi)[B_i\,\mathrm{sec}h(\xi) + d_i\tan h(\xi)] + B_0}. \tag{13}$$

Equation (13) may be rewritten with the help of Equations (9) and (10) as following:

$$U(\omega) = \frac{\sum_{i=1}^{n}\cos^{i-1}(\omega)[A_i\sin(\omega) + c_i\cos(\omega)] + A_0}{\sum_{i=1}^{m}\cos^{i-1}(\omega)[B_i\sin(\omega) + d_i\cos(\omega)] + B_0}, \tag{14}$$

in which the values of n, m will be determined later via balance principle. After putting the necessary derivations of Equation (14) into Equation (12), we obtain an equation of $\sin^i(\omega)\cos^j(\omega)$. Taking all these terms to zero yields a system of equations. Solving this system by using some computational programs, gives the values of A_i, B_i, c_i, d_i, μ, and c. Via these values of parameters A_i, B_i, c_i, d_i, μ, and c in Equation (13), we obtain the new traveling wave solutions to Equation (11).

3. Applications of Projected Scheme

In this part of the paper, the stationary soliton and new analytical solutions to the Riemann wave system and conformable GPE is studied by using RSGEM.

3.1. RSGEM to the Riemann Wave System of Equations. First of all, we apply RSGEM to the Riemann wave system of equations for reporting new stationary soliton solutions. Applying the traveling wave transformation defined by

$$\begin{aligned} u(x,y,t) &= U(\xi), \xi = \mu x + \delta y - \omega t,\\ V(x,y,t) &= V(\xi),\\ \Psi(x,y,t) &= \Psi(\xi), \end{aligned} \tag{15}$$

into Equation (1) results in the following NODE:

$$2\alpha\delta\mu^2 V'' - 2\omega V + (\beta\mu + \gamma\delta)V^2 = 0, \tag{16}$$

where

$$\begin{aligned} U(\xi) &= \frac{\delta}{\mu}V(\xi),\\ \Psi(\xi) &= \frac{\mu}{\delta}V(\xi). \end{aligned} \tag{17}$$

After taking $n = m$ especially in this paper, via the balance rule in Equation (16) gives $n = m = 2$. Getting $n = m = 2$ in Equation (14), one can write the trial equation of solution function given as follows:

$$V(w) = \frac{A_0 + A_1\sin(w) + c_1\cos(w) + \cos(w)[A_2\sin(w) + c_2\cos(w)]}{B_0 + B_1\sin(w) + d_1\cos(w) + \cos(w)[B_2\sin(w) + d_2\cos(w)]}. \tag{18}$$

Substituting Equation (18) and its second derivative into Equation (16), we obtain an equation of $\sin^i(w)\cos^i(w)$. Getting all coefficients of these terms to zero, we gain a system of equations. Solving this system produces the values of parameters $A_i, B_i, c_1, d_1, \mu, \omega$, and δ which results in many entirely new traveling wave solutions to the Equation (1).

Case-1: when $B_2 = d_2 = 0, b_1 = -2, B_0 = 1, \omega = A_0 = -b_0, A_1 = -b_0B_1, A_2 = \frac{3ib_0}{2}, c_1 = \frac{1}{2}ib_0B_1, c_2 = \frac{3b_0}{2}, d_1 = iB_1$ into Equation (13) with $n = 2$, it yields the following entirely complex mixed dark–bright soliton solution to the RWE as follows

$$V_1 = \frac{-\kappa - \kappa B_1\mathrm{sec}h[f(x,y,t)] + \frac{1}{2}i\kappa B_1\tan h[f(x,y,t)] + \tan h[f(x,y,t)]g}{1 + B_1\mathrm{sec}h[f(x,y,t)] + iB_1\tan h[f(x,y,t)]}, \tag{19}$$

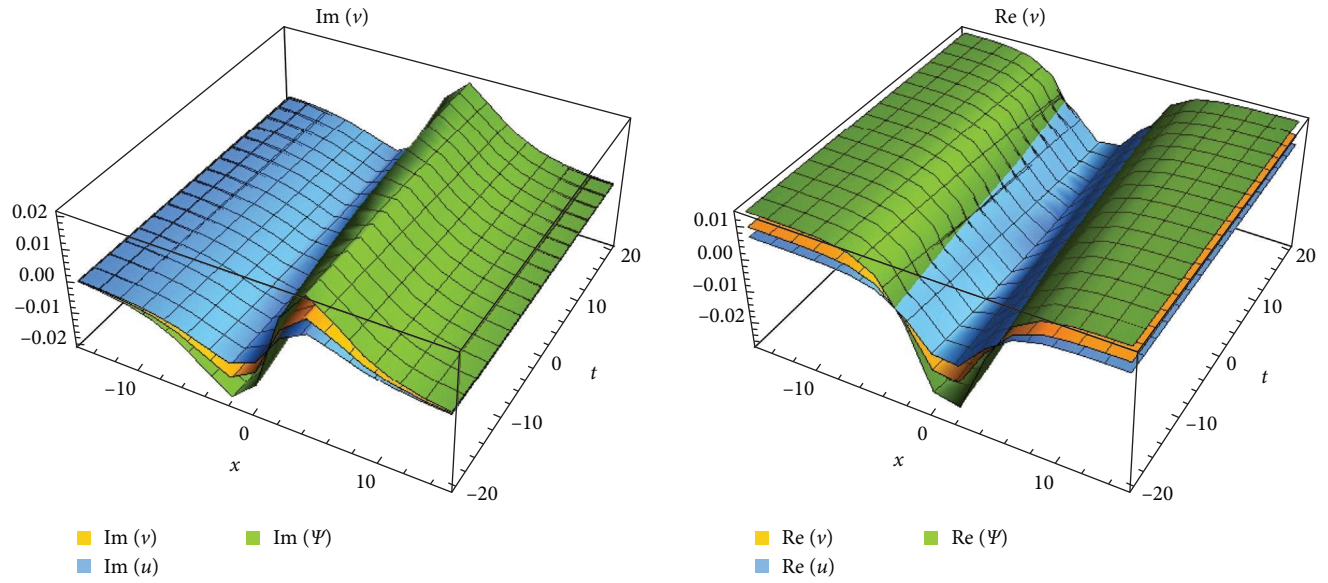

FIGURE 1: The 3D simulations of V_1.

$$U_1 = \frac{\delta\left(-\kappa - \kappa B_1 \operatorname{sech}[f(x,y,t)] + \frac{1}{2} i\kappa B_1 \tanh[f(x,y,t)] + \tanh[f(x,y,t)]g\right)}{\mu(1 + B_1 \operatorname{sech}[f(x,y,t)] + iB_1 \tanh[f(x,y,t)])}, \tag{20}$$

$$\Psi_1 = \frac{\mu\left(-\kappa - \kappa B_1 \operatorname{sech}[f(x,y,t)] + \frac{1}{2} i\kappa B_1 \tanh[f(x,y,t)] + \tanh[f(x,y,t)]g\right)}{\delta(1 + B_1 \operatorname{sech}[f(x,y,t)] + iB_1 \tanh[f(x,y,t)])}, \tag{21}$$

where $V_1 = V_1(x,y,t), U_1 = U_1(x,y,t), \Psi_1 = \Psi_1(x,y,t), \kappa = \alpha\delta\mu^2, f(x,y,t) = \delta y + \mu x + \kappa t, g = g(x,y,t) = \frac{3}{2} i\kappa \operatorname{sech}[f(x,y,t)] + \frac{3}{2} i\kappa \tanh[f(x,y,t)]$. Selecting several parameters values from the physical meanings of the RWE, we can observe the simulations of Equation (19) via Figure 1 in 3D, Figure 2 contour sense, and Figure 3 in 2D according to the specific time scala. From these simulations, one can see that this solution has singular properties.

Case-2: choosing as $B_2 = d_2 = 0, b_1 = -2, B_0 = 1, \omega = A_0 = -b_0, A_1 = -b_0 B_1, A_2 = -\frac{3ib_0}{2}, c_1 = -\frac{1}{2} ib_0 B_1, c_2 = \frac{3b_0}{2}, d_1 = -iB_1$; for Equation (13) with $n = 2$, it produces entirely new complex mixed dark–bright soliton solution given by

$$V_2 = \frac{-\kappa - \kappa B_1 \operatorname{sech}[f(x,y,t)] - \frac{1}{2} i\kappa B_1 \tanh[f(x,y,t)] + \tanh[f(x,y,t)]g}{1 + B_1 \operatorname{sech}[f(x,y,t)] - iB_1 \tanh[f(x,y,t)]}, \tag{22}$$

$$U_2 = \frac{\delta\left(-\kappa - \kappa B_1 \operatorname{sech}[f(x,y,t)] - \frac{1}{2} i\kappa B_1 \tanh[f(x,y,t)] + \tanh[f(x,y,t)]g\right)}{\mu(1 + B_1 \operatorname{sech}[f(x,y,t)] - iB_1 \tanh[f(x,y,t)])}, \tag{23}$$

$$\Psi_2 = \frac{\mu\left(-\kappa - \kappa B_1 \operatorname{sech}[f(x,y,t)] - \frac{1}{2} i\kappa B_1 \tanh[f(x,y,t)] + \tanh[f(x,y,t)]g\right)}{\delta(1 + B_1 \operatorname{sech}[f(x,y,t)] - iB_1 \tanh[f(x,y,t)])}, \tag{24}$$

where $V_2 = V_2(x,y,t), U_2 = U_2(x,y,t), \Psi_2 = \Psi_2(x,y,t), \kappa = \alpha\delta\mu^2, f(x,y,t) = \delta y + \mu x + \kappa t, g = g(x,y,t) = -\frac{3}{2} i\kappa \operatorname{sech}[f(x,y,t)] + \frac{3}{2} i\kappa \tanh[f(x,y,t)]$. More strict simulations of Equations (22)–(26) are also seen by Figure 4 in three-dimensional,

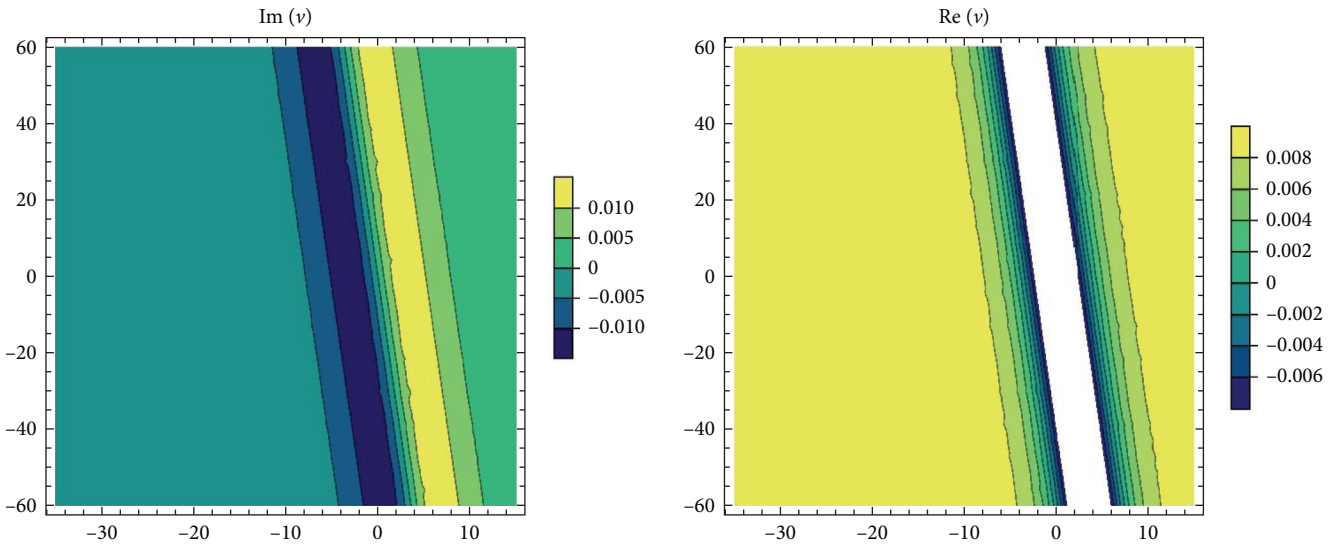

Figure 2: The contour simulations of V_1.

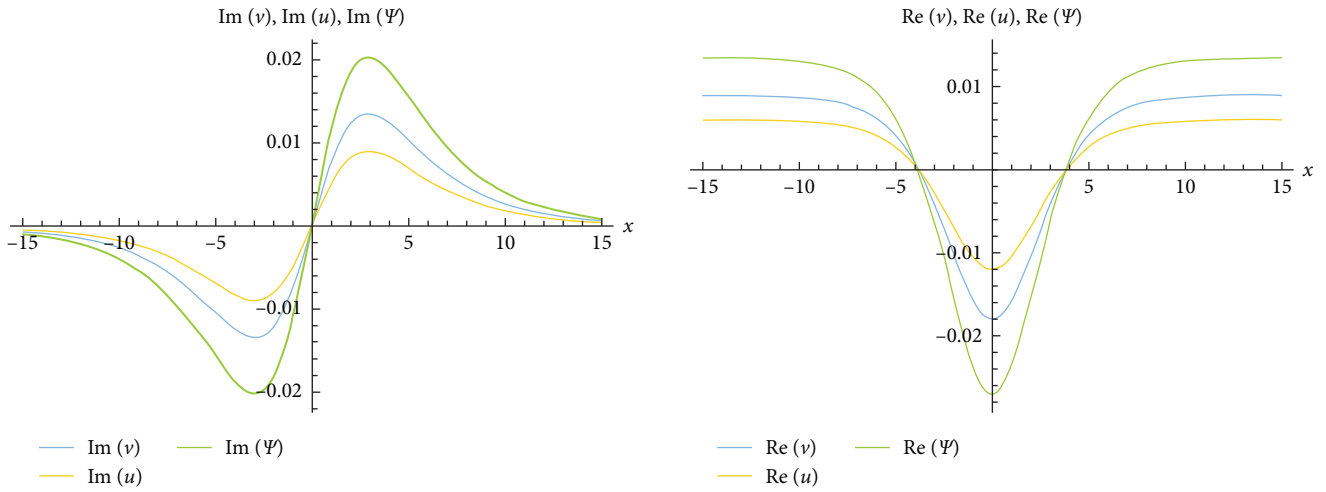

Figure 3: The 2D simulations of V_1.

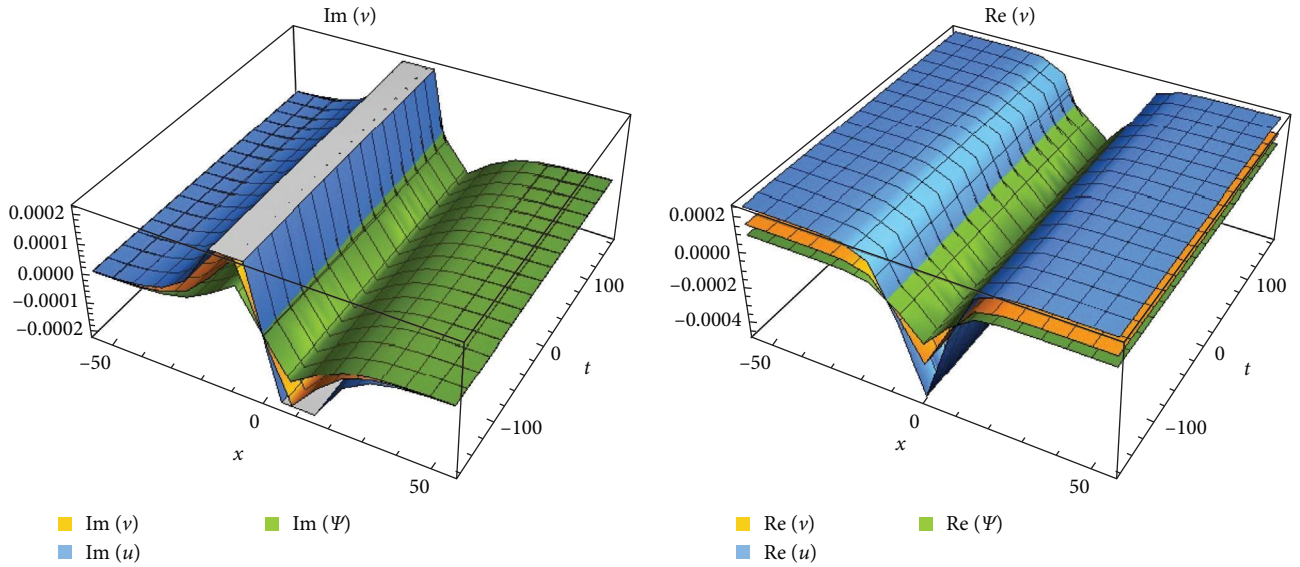

Figure 4: The 3D simulations of V_2.

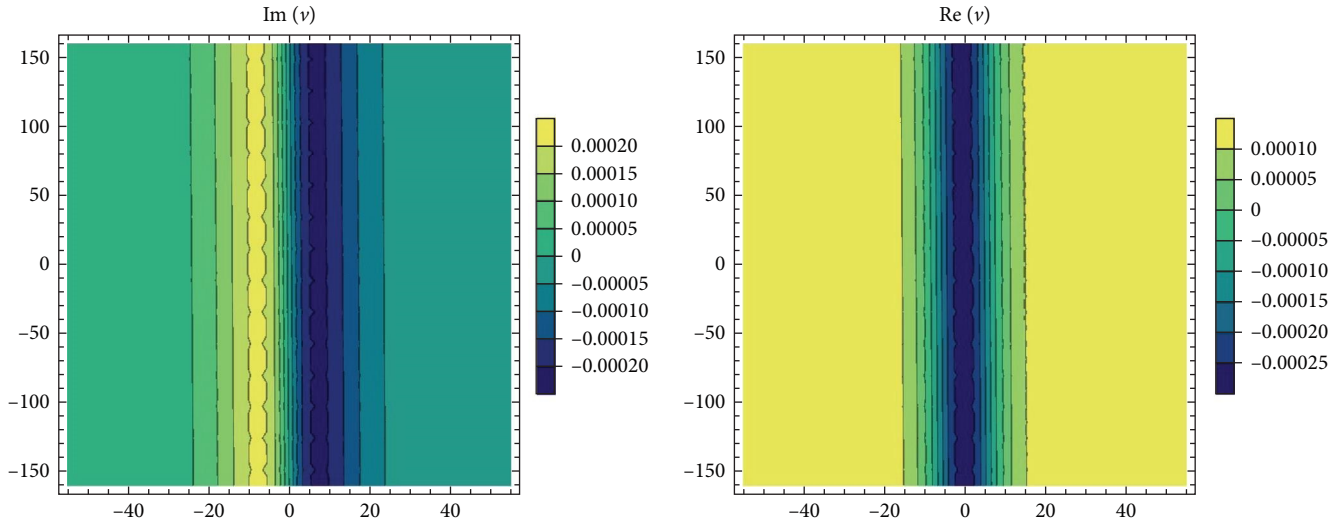

Figure 5: The contour simulations of V_2.

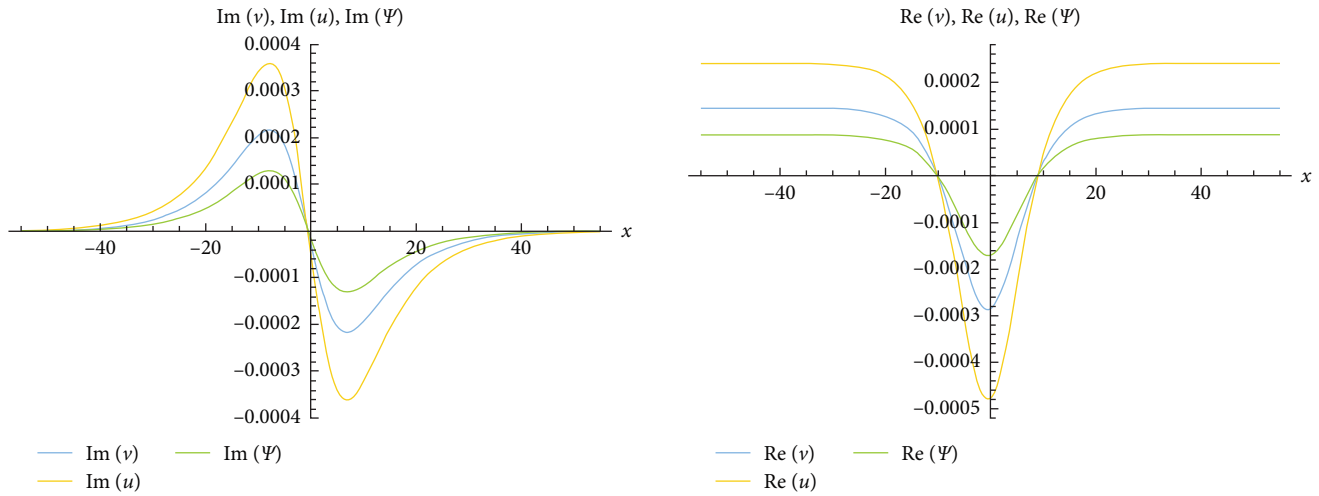

Figure 6: The 2D simulations of V_2.

Figure 5 contour sense, and Figure 6 in two-dimensional in a specific time. From the Figures 4 to –6, it may be observed that this solution has dark–bright properties.

Case-3: once it is selected as $B_2 = d_2 = 0, b_1 = -2, B_0 = 1, \omega = -b_0, A_0 = \frac{b_0}{2}, A_1 = -b_0 B_1, A_2 = 0, c_1 = \frac{1}{2} b_0 \sqrt{1 - B_1^2}$, $c_2 = 0, d_1 = \sqrt{1 - B_1^2}$ for Equation (13) with $n = 2$, and inserting these values into Equation (13) along with $n = 2$, we obtain dark–bright soliton solution as following:

$$V_3(x,y,t) = \frac{\frac{1}{2}\kappa - \kappa B_1 \operatorname{sech}[f(x,y,t)] + \frac{1}{2}\kappa\sqrt{1 - B_1^2}\tanh[f(x,y,t)]}{1 + B_1 \operatorname{sech}[f(x,y,t)] + \sqrt{1 - B_1^2}\tanh[f(x,y,t)]}, \tag{25}$$

$$U_3(x,y,t) = \frac{\delta\left(\frac{1}{2}\kappa - \kappa B_1 \operatorname{sech}[f(x,y,t)] + \frac{1}{2}\kappa\sqrt{1 - B_1^2}\tanh[f(x,y,t)]\right)}{\mu\left(1 + B_1 \operatorname{sech}[f(x,y,t)] + \sqrt{1 - B_1^2}\tanh[f(x,y,t)]\right)}, \tag{26}$$

$$\Psi_3(x,y,t) = \frac{\mu\left(\frac{1}{2}\kappa - \kappa B_1 \operatorname{sech}[f(x,y,t)] + \frac{1}{2}\kappa\sqrt{1 - B_1^2}\tanh[f(x,y,t)]\right)}{\delta\left(1 + B_1 \operatorname{sech}[f(x,y,t)] + \sqrt{1 - B_1^2}\tanh[f(x,y,t)]\right)}, \tag{27}$$

where $\kappa = \alpha\delta\mu^2, f(x,y,t) = \delta y + \mu x + \kappa t$. Moreover, $-1 < B_1 < 1$ for strain condition. The intersection points of Equations (25)–(27) are also observed by Figure 7 in three- and two-dimensional in a specific time and Figure 8 in the low region. From the Figures 7 and 8, it may be also seen that Equations (25)–(27) have singular property.

Case-4: if it is chosen as $\omega = b_0, B_2 = d_2 = 0, b_1 = -2$, $B_0 = 1$, $A_0 = -\frac{b_0}{2}$, $A_1 = -\frac{1}{2} b_0 B_1$, $A_2 = 0$, $c_1 = 0, d_1 = -1$, mixed-dark soliton solution to the Equation (1) is obtained as following

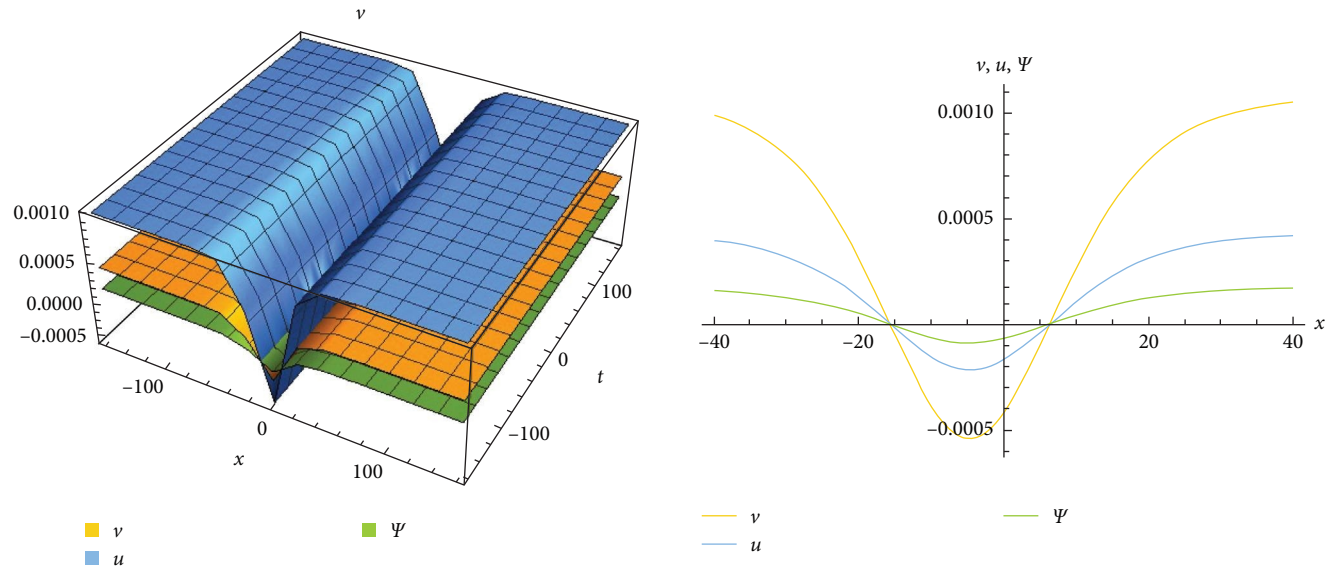

FIGURE 7: The 3D and 2D simulations of V_3.

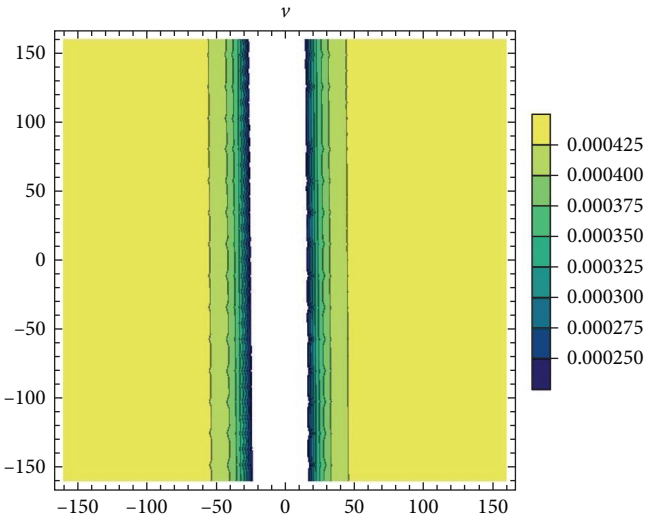

FIGURE 8: The contour simulation of V_3.

$$V_4(x,y,t)=\frac{-\frac{1}{2}\kappa-\frac{1}{2}\kappa B_1\operatorname{sech}[f(x,y,t)]+\frac{1}{2}\kappa\tanh[f(x,y,t)]}{1+B_1\operatorname{sech}[f(x,y,t)]-\tanh[f(x,y,t)]}, \tag{28}$$

$$U_4(x,y,t)=\frac{\delta\left(-\frac{1}{2}\kappa-\frac{1}{2}\kappa B_1\operatorname{sech}[f(x,y,t)]+\frac{1}{2}\kappa\tanh[f(x,y,t)]\right)}{\mu(1+B_1\operatorname{sech}[f(x,y,t)]-\tanh[f(x,y,t)])}, \tag{29}$$

$$\Psi_4(x,y,t)=\frac{\mu\left(-\frac{1}{2}\kappa-\frac{1}{2}\kappa B_1\operatorname{sech}[f(x,y,t)]+\frac{1}{2}\kappa\tanh[f(x,y,t)]\right)}{\delta(1+B_1\operatorname{sech}[f(x,y,t)]-\tanh[f(x,y,t)])}, \tag{30}$$

where $\kappa=\alpha\delta\mu^2, f(x,y,t)=\delta y+\mu x+\kappa t$, and also δ, μ, α, B_1 are real constants and nonzero. The periodic wave behaviors of Equations (28)–(30) may be also presented by Figure 9. Figure 9 has stable wave propagation.

Case-5: when $\alpha=\frac{A_2}{3\delta\mu^2}, \beta=\frac{2-\gamma\delta}{\mu}, B_2=d_2=0, b_1=1, B_0=i, A_0=\frac{2iA_2}{3}, \omega=\frac{-A_2}{3}, A_1=-\frac{2}{3}iA_2d_1, B_1=-id_1, c_1=-\frac{1}{3}A_2d_1, b_0=\frac{A_2}{3}, c_2=-iA_2$ results in the another entirely new exact solution as follows:

$$V_5=\frac{\frac{2iA_2}{3}-\frac{2}{3}iA_2d_1\operatorname{sech}(f)-\frac{1}{3}A_2d_1p+\tanh(f)(A_2\tanh(f)-iA_2\tanh(f))}{i-id_1\operatorname{sech}(f)+d_1\tanh(f)}, \tag{31}$$

$$U_5=\frac{\delta\left(\frac{2iA_2}{3}-\frac{2}{3}iA_2d_1\operatorname{sech}(f)-\frac{1}{3}A_2d_1p+\tanh(f)(A_2\operatorname{sech}(f)-iA_2\tanh(f))\right)}{\mu(i-id_1\operatorname{sech}(f)+d_1\tanh(f))}, \tag{32}$$

$$\Psi_5=\frac{\mu\left(\frac{2iA_2}{3}-\frac{2}{3}iA_2d_1\operatorname{sech}(f)-\frac{1}{3}A_2d_1p+\tanh(f)(A_2\operatorname{sech}(f)-iA_2\tanh(f))\right)}{\delta(i-id_1\operatorname{sech}(f)+d_1\tanh(f))}, \tag{33}$$

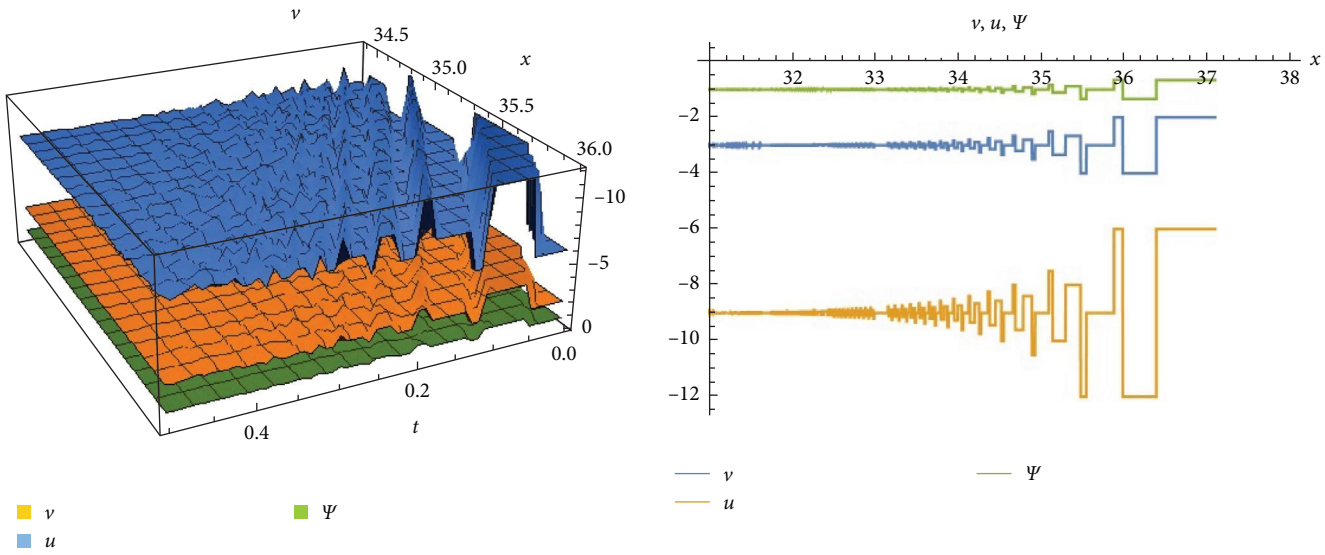

FIGURE 9: The 3D and 2D simulations of V_4.

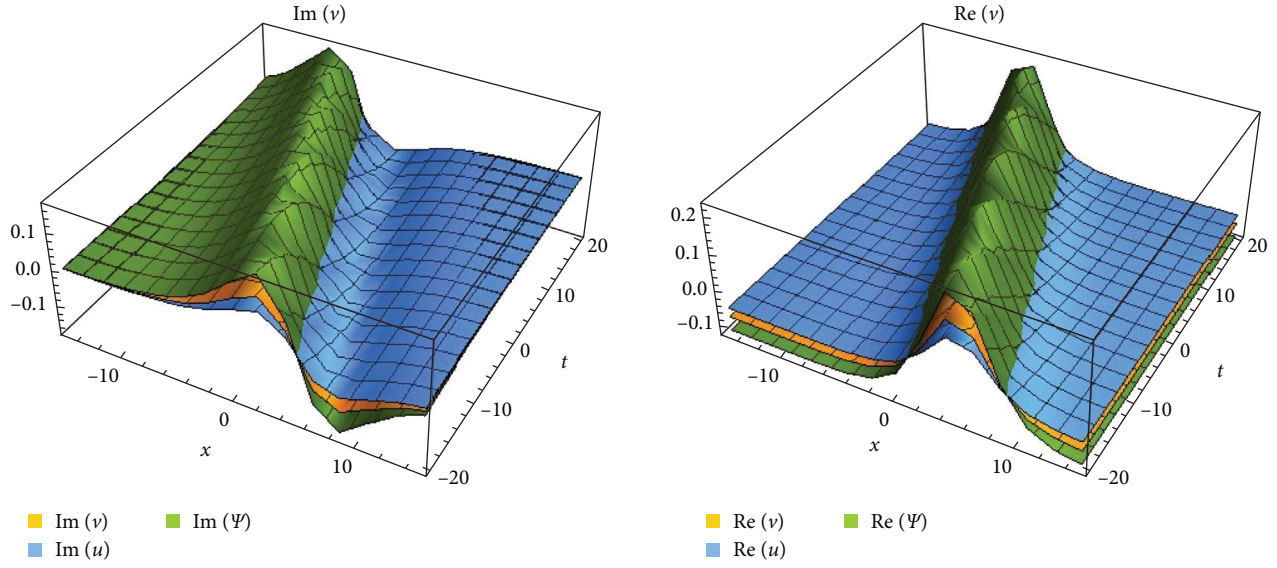

FIGURE 10: The 3D simulations of V_5.

where $f = f(x, y, t) = \tanh(\delta y + \mu x + \frac{A_2}{3} t)$, and also δ, μ, A_2, d_1 are real constants and nonzero. Smooth wave distribution of Equations(31)–(33) are also plotted by Figure 10 in three-dimensional, Figure 11 contour sense, and Figure 12 in two-dimensional in a specific time. From the Figures 10–12, these solution have the dark–bright properties.

Case-6: using $\alpha = \frac{A_2}{3\delta\mu^2}, \beta = \frac{2-\gamma\delta}{\mu}, B_2 = d_2 = 0, b_1 = 1, B_0 = i, \omega = -\frac{A_2}{3}, A_0 = -iA_2, A_1 = 0, B_1 = 0, c_1 = 0, b_0 = -\frac{A_2}{3}, c_2 = iA_2, d_1 = 0$ produces combined dark–bright stationary soliton solution as follows:

$$V_6 = -A_2 - i\tanh(\delta y + \mu x + \varpi t)(A_2 \operatorname{sech}(\delta y + \mu x + \varpi t) + iA_2 \tanh(\delta y + \mu x + \varpi t)), \tag{34}$$

$$U_6 = \frac{\delta}{\mu}(-A_2 - i\tanh(\delta y + \mu x + \varpi t)(A_2 \operatorname{sech}(\delta y + \mu x + \varpi t) + iA_2 \tanh(f))), \tag{35}$$

$$\Psi_6 = \frac{\mu}{\delta}(-A_2 - i\tanh(\delta y + \mu x + \varpi t)(A_2 t \operatorname{sech}(\delta y + \mu x + \varpi t) + iA_2 \tanh(f))), \tag{36}$$

where $f = \delta y + \mu x + \varpi t)$, $\varpi = \frac{A_2}{3}$ and δ, μ, A_2 are real constants and nonzero. Intercrossing wave distribution of Equations (34)–(36) are also introduced by Figures 13 and 14. Such sketches is estimated that soliton wavelength is closely

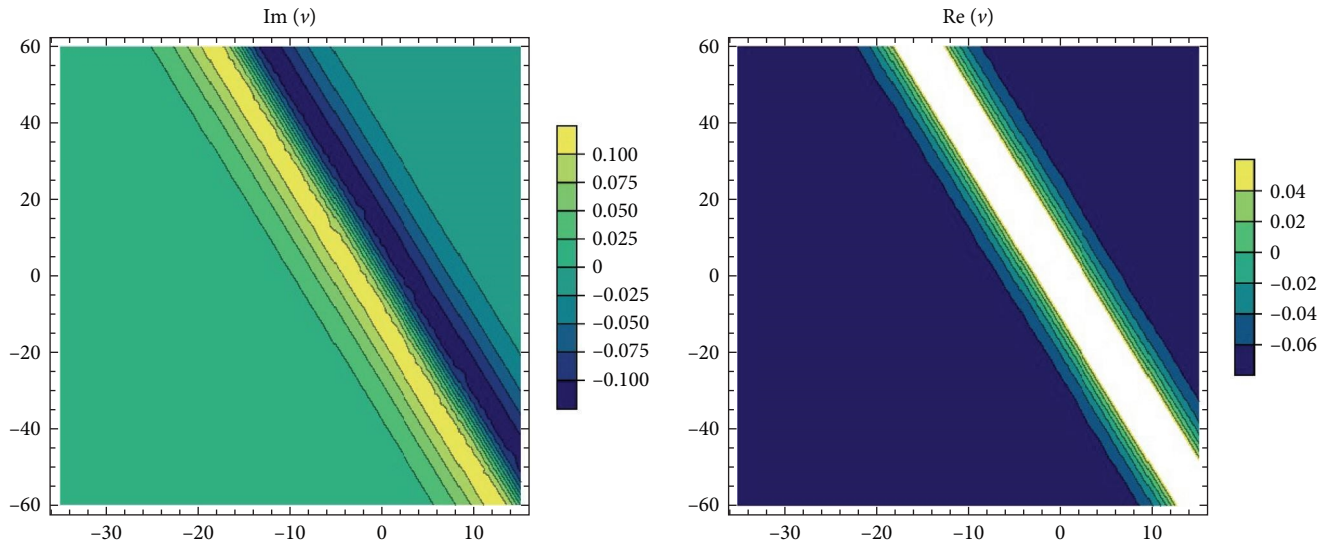

Figure 11: The contour simulations of V_5.

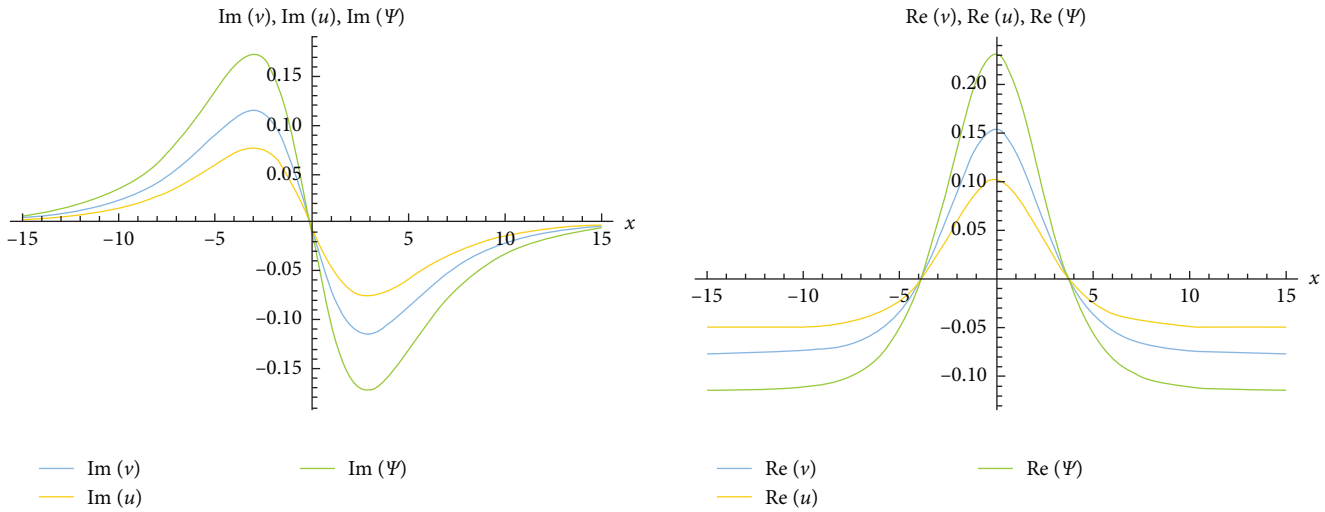

Figure 12: The 2D simulations of V_5.

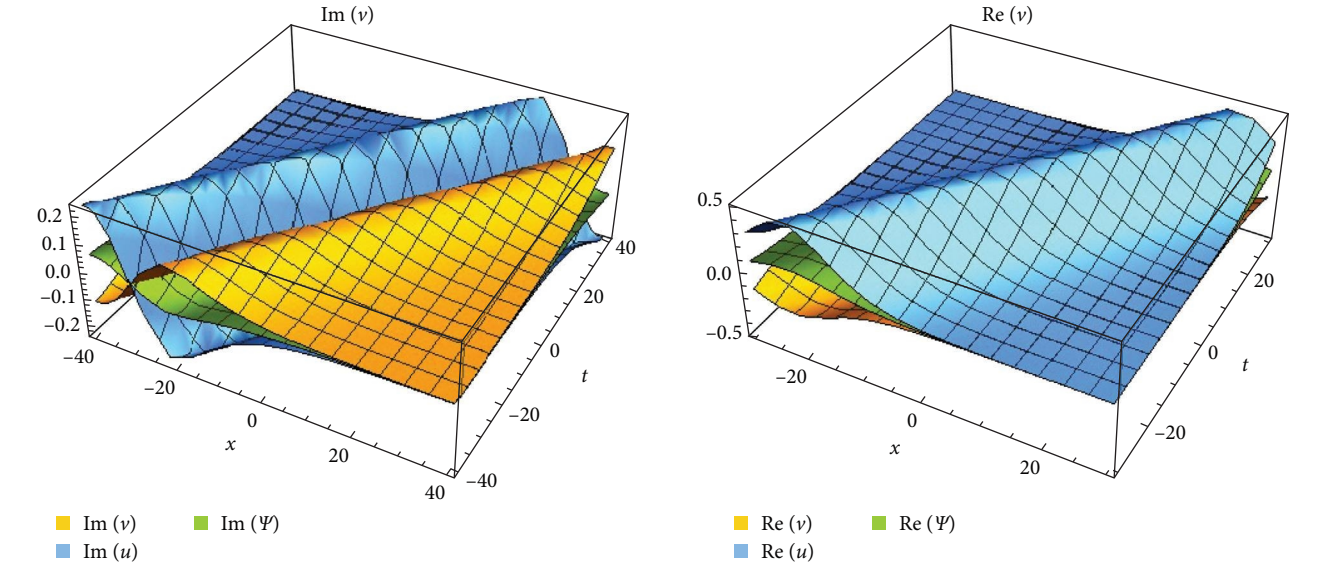

Figure 13: The 3D simulations of V_6.

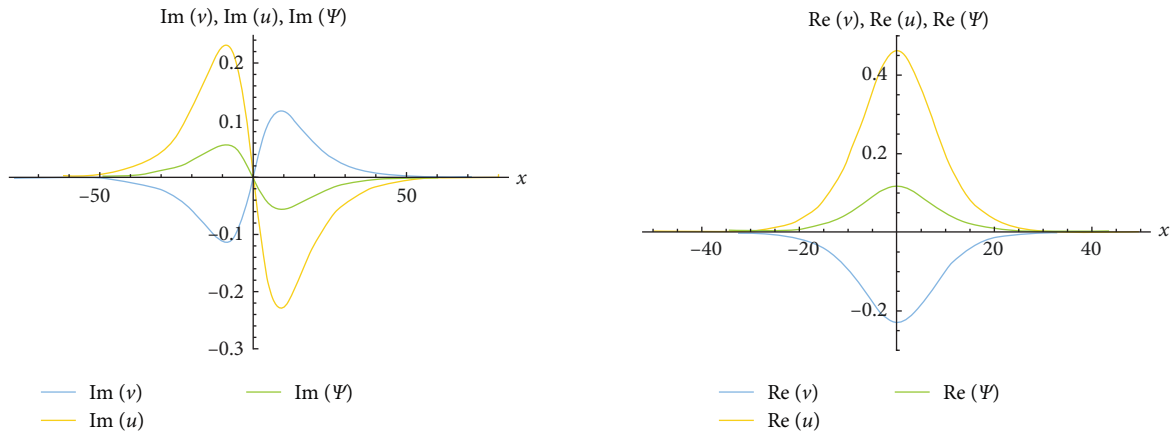

FIGURE 14: The 2D simulations of V_6.

related to the gravitational potential. Thus, it may be said that the gravitational potential affect the wavelength and its power. From the Figures 13 and 14, it is estimated that they may be used to explain the gravitational potential energy properties.

3.2. RSGEM for the Nonlinear GPE in Conformable Operator. This subsection of the manuscript extracts the stationary soliton, mixed dark–bright and complex traveling wave solutions to the conformable GPE by using RSGEM. Applying wave transform given as follows:

$$q(X,T) = U(\xi)e^{i\varphi}, \xi = \alpha X - \frac{\beta}{\theta}T^{\theta}, \varphi = pX - \frac{\kappa}{\theta}T^{\theta}, \tag{37}$$

in which α, β, κ are nonzero and also $0<\theta<1$ into Equation (4) converts

$$\alpha^2 U'' + (2\kappa - p^2)U - 2\Upsilon U^3 = 0. \tag{38}$$

Here Υ is a real constant. Considering balance properties in Equation (38), we find $n=1$ for Equations (13) and (14). Using $n=1$ Equation (14) reaches the following trial solution function given as:

$$U(w) = \frac{A_0 + A_1\sin(w) + c_1\cos(w)}{B_0 + B_1\sin(w) + d_1\cos(w)}, \tag{39}$$

where B_1, d_1 are each nonzero constants. Putting Equation (39) and its second derivation in Equation (38) gives various terms containing $\sin^s(w)\cos^s(w)$. This produces a system of algebraic equations. Solving this system, we find the desired analytical solutions as follows to the conformable GPE.

Case-1: using $B_1 = -id, c_1 = iA_1, \Upsilon = \frac{-\alpha^2 d_1^2}{4A_1^2}, B_0 = -\frac{iA_0 d_1}{A_1}, \kappa = \frac{1}{4}(\alpha^2 + 2p^2)$ produces mixed dark–bright stationary soliton solution as follows:

$$q_1(X,T) = \frac{e^{i\left(pX - \frac{(\alpha^2+2p^2)}{4\theta}T^{\theta}\right)}\left(A_0 + A_1\operatorname{sech}\left(\alpha X - \frac{\alpha p}{\theta}T^{\theta}\right) + iA_1\tanh\left(\alpha X - \frac{\alpha p}{\theta}T^{\theta}\right)\right)}{-id_1\operatorname{sech}\left(\alpha X - \frac{\alpha p}{\theta}T^{\theta}\right) - \frac{iA_0 d_1}{A_1} + d_1\tanh\left(\alpha X - \frac{\alpha p}{\theta}T^{\theta}\right)}, \tag{40}$$

where $\alpha, A_0, A_1, p, d_1, 0<\theta<1$ are real constants and nonzero. Selecting suitable to the physical properties of conformable GPE, we plot various wave distributions Figure 15. From the Figure 15, it is estimated that it has mixed dark–bright stationary.

3.3. Stability Properties of $q_1(X,T)$. In this subsection of this paper, Hamiltonian system is considered and applied on the mixed dark–bright stationary soliton solution to investigate its stability on a general range. This system is introduced in detail [71, 72] as following

$$\Pi(w) = \int_{-\infty}^{\infty} \frac{1}{2}\Psi^2(\zeta)d\zeta, \tag{41}$$

in which Π symbolizes the momentum function and also w is used to express the wave speed and $\Psi(\zeta)$ is the projected analytical solution. Sandstede et al. [72] observed some important models by using various spaces properties such as Banach and so on. The sufficient condition for the stability is as follows:

$$\frac{\partial \Pi}{\partial w} > 0. \tag{42}$$

If we take into account Equations (41), and (42) on Equation (40), we obtain

$$\frac{\partial \Pi}{\partial w} = \frac{1}{\sqrt{2}d_1^2}\left(\frac{1}{2} + \frac{i}{2}\right)(-1)^{\frac{3}{4}}A_1^2 e^{-\frac{i\alpha^2}{2\theta}t^{\theta} + p^2\left(-\frac{i}{\theta}t^{\theta} + \frac{2i}{\lambda}\right) + t\lambda - \frac{i(-2p+\lambda x)^2}{2\lambda}} > 0. \tag{43}$$

Thus, the Equation (40) solution is unconditionally stable.

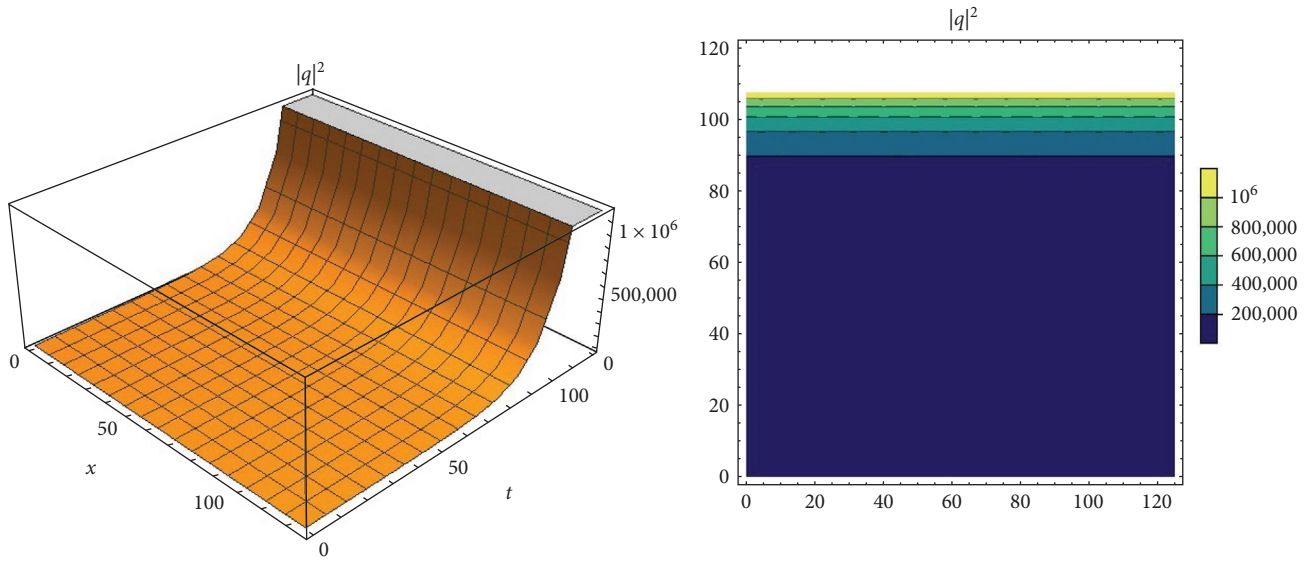

FIGURE 15: The 3D and contour simulations of $q_1(X, T)$.

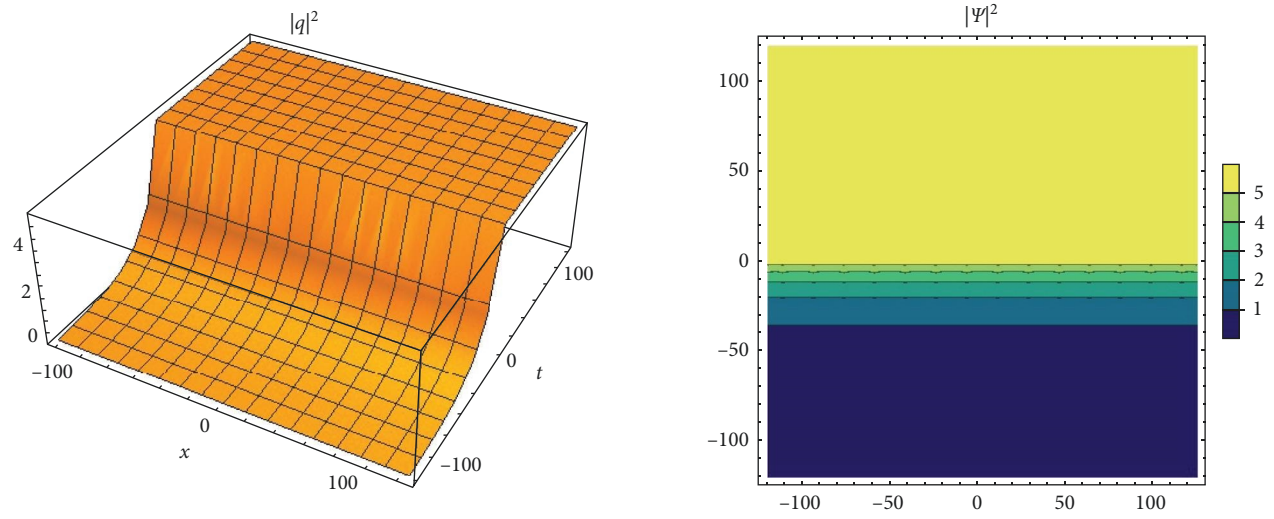

FIGURE 16: The 3D and contour simulations of $q_2(X, T)$.

Case-2: when $B_1 = \frac{A_0 d_1}{A_1}, c_1 = \frac{A_1^2}{A_0}, \Upsilon = \frac{(2\kappa - p^2)A_0^2 d_1^2}{2A_1^4}, B_0 = \frac{A_0^2 d_1}{A_1^2}$ reaches the mixed dark–bright stationary soliton solution as follows:

$$q_2(X,T) = \frac{e^{i\left(pX - \frac{\kappa}{\theta}T^\theta\right)}\left(A_0 + A_1 \operatorname{sech}\left(\alpha X - \frac{\alpha p}{\theta}T^\theta\right) + \frac{A_1^2}{A_0}\tanh\left(\alpha X - \frac{\alpha p}{\theta}T^\theta\right)\right)}{\frac{A_0^2 d_1}{A_1^2} + \frac{A_0 d_1}{A_1}\operatorname{sech}\left(\alpha X - \frac{\alpha p}{\theta}T^\theta\right) + d_1 \tanh\left(\alpha X - \frac{\alpha p}{\theta}T^\theta\right)}, \tag{44}$$

where $p, \alpha, A_0, A_1, d_1, \kappa, 0 < \theta < 1$ are real constants and nonzero. With the suitable values related to the physical properties for governing model, various wave distributions may be observed Figure 16. From the Figure 16, it is estimated that it has some important wave propagations.

3.4. Stability Properties of $q_2(X, T)$. Here, if we reconsider the momentum function as follows:

$$\Pi(w) = \int_{-\infty}^{\infty} \frac{1}{2}\Psi^2(\zeta)d\zeta, \tag{45}$$

and the sufficient condition for the stability condition by

$$\frac{\partial \Pi}{\partial w} > 0, \tag{46}$$

on Equation (44), we obtain

$$\frac{\partial \Pi}{\partial w} = \frac{A_1^4 e^{2ipx - \frac{2i\kappa}{\theta}t^\theta}}{2A_0^2 d_1^2} > 0, \tag{47}$$

which is the mixed dark–bright stationary soliton solution given as Equation (44) is unconditionally stable.

4. Modulation Instability Analysis of the Nonlinear GPE

In this section of the article, we discuss the modulation instability (MI) analysis for the stationary solutions of Equation (4) by assuming the following stationary solutions

$$q(X,T)=\left(\sqrt{\Omega}+\Xi(X,T)\right)e^{i\Omega X}, \tag{48}$$

where Ω represents the incident power. We investigate the evolution of the perturbation $\Xi(X,T)$ using the concept of linear stability analysis. Substituting Equation (48) into Equation (4) and linearizing the result in $\Xi(X,T)$, we acquire

$$i\partial_T\Xi(X,T)+\frac{1}{2}\partial_{X,X}\Xi(X,T)-\gamma(|\Xi(X,T)|)^2\Xi(X,T)=0, \tag{49}$$

supposing solutions of Equation (49) are in the following

$$\Xi(X,T)=\xi e^{i(\beta x-\alpha t)}+\zeta e^{-i(\beta x-\alpha t)}, \tag{50}$$

where β is the wave number, and α is the frequency. Putting Equation (50) in Equation (49) gives a set of two homogenous equations as follows:

$$\alpha\zeta-\frac{1}{2}\beta^2\zeta-3\gamma\zeta^2\xi-\gamma\zeta^3=0, \tag{51}$$

$$-\alpha\xi-\frac{1}{2}\beta^2\xi-3\gamma\zeta\xi^2-\gamma\xi^3=0. \tag{52}$$

From the Equations (51) and (52), one can easily obtain the following coefficients matrix of ζ and ξ as follows:

$$\begin{pmatrix} -3\gamma\zeta^2 & \alpha-\frac{1}{2}\beta^2-\gamma\zeta^2 \\ -\alpha-\frac{1}{2}\beta^2-\gamma\xi^2 & -3\gamma\xi^2 \end{pmatrix}\begin{pmatrix}\xi\\ \zeta\end{pmatrix}=\begin{pmatrix}0\\0\end{pmatrix}. \tag{53}$$

The coefficient matrix in Equation (53) has a nontrivial solution if the determinant equal to zero. By expanding the determinant, we obtain the following

$$\alpha^2-\frac{1}{4}\beta^4+8\gamma^2\zeta^2\xi^2+\alpha\gamma(-\zeta^2+\xi^2)-\frac{1}{2}\beta^2\gamma(\zeta^2+\xi^2)=0. \tag{54}$$

Equation (54) has the following solutions

$$\beta=\mp\sqrt{-\gamma(\zeta^2+\xi^2)-\sqrt{(-2\alpha+\gamma\zeta^2)^2+2\gamma(2\alpha+17\gamma\zeta^2)\xi^2+\gamma^2\xi^4}}, \tag{55}$$

and

$$\beta=\mp\sqrt{-\gamma(\zeta^2+\xi^2)+\sqrt{(-2\alpha+\gamma\zeta^2)^2+2\gamma(2\alpha+17\gamma\zeta^2)\xi^2+\gamma^2\xi^4}}. \tag{56}$$

The stability of the steady state is determined by Equations (55) and (56). If the wave number has an imaginary part, the steady-state solution is unstable since the perturbation grows exponentially. But if the wave number is real, the steady state is stable against small perturbation. Thus, the condition is necessary for the existence of MI to occur from Equations (55) and (56) is when either

$$\gamma(\zeta^2+\xi^2)+\sqrt{(-2\alpha+\gamma\zeta^2)^2+2\gamma(2\alpha+17\gamma\zeta^2)\xi^2+\gamma^2\xi^4}>0, \tag{57}$$

or

$$-\gamma(\zeta^2+\xi^2)+\sqrt{(-2\alpha+\gamma\zeta^2)^2+2\gamma(2\alpha+17\gamma\zeta^2)\xi^2+\gamma^2\xi^4}<0. \tag{58}$$

Now for investigating instability modulation gain spectrum it should be noticed that

$$g(\alpha)=2\mathrm{Im}(\beta)=\mp2\sqrt{-\gamma(\zeta^2+\xi^2)+\sqrt{(-2\alpha+\gamma\zeta^2)^2+2\gamma(2\alpha+17\gamma\zeta^2)\xi^2+\gamma^2\xi^4}}. \tag{59}$$

We have the following cases

Case 1: when

$$g(\alpha)=2\mathrm{Im}(\beta)=2\sqrt{-\gamma(\zeta^2+\xi^2)+\sqrt{(-2\alpha+\gamma\zeta^2)^2+2\gamma(2\alpha+17\gamma\zeta^2)\xi^2+\gamma^2\xi^4}}. \tag{60}$$

We have the following subcases

Case 1.1: for these values $\gamma=\frac{-2}{3}$, $\zeta=\frac{2}{5}$, $\xi=\frac{1}{2}$, of constants in Equation (59) we have

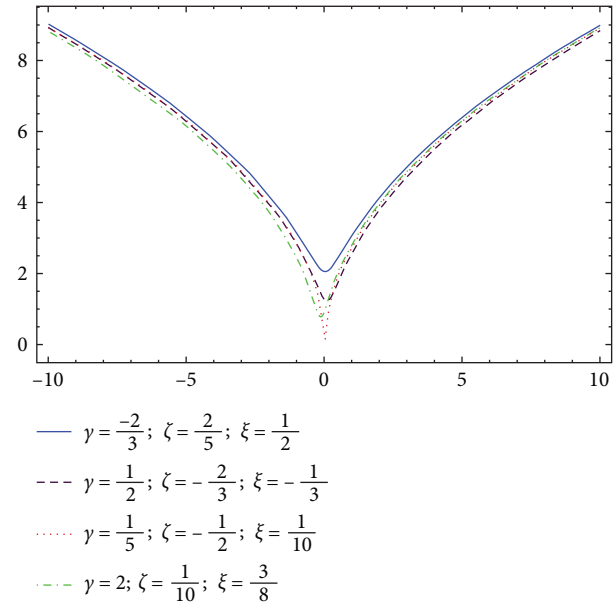

FIGURE 17: The instability modulation gain spectra in the normal-GVD regime where $-10<\alpha<10$, and for different values mentioned at legends.

$$g_{1,1}(\alpha)=\frac{1}{5}\sqrt{\frac{82}{3}+2\sqrt{1,609+200\alpha(-3+50\alpha)}}. \tag{61}$$

Case 1.2: when it is considered as $\gamma=\frac{1}{2},\zeta=\frac{-2}{3},\xi=\frac{-1}{3}$, of constants in Equation (59) we have

$$g_{1,2}(\alpha)=\frac{1}{3}\sqrt{-10+6\sqrt{17+24\alpha(-1+6\alpha)}}. \tag{62}$$

Case 1.3: taking as $\gamma=\frac{1}{5},\zeta=\frac{-1}{2},\xi=\frac{1}{10}$, of constants in Equation (59) we have

$$g_{1,3}(\alpha)=\frac{1}{5}\sqrt{\frac{2}{5}}\sqrt{-13+\sqrt{369+200\alpha(-6+125\alpha)}}. \tag{63}$$

Case 1.4: once they are considered as $\gamma=2,\zeta=\frac{1}{10},\xi=\frac{3}{8}$ of constants in Equation (59) we have

$$g_{1,4}(\alpha)=\frac{1}{10\sqrt{2}}\sqrt{-241+\sqrt{173,281+3,200\alpha(209+800\alpha)}}. \tag{64}$$

These subcases can be expressed in Figure 17 between $-10<\alpha<10$.

5. Conclusions

In this work, we introduced a recently developed scheme being RSGEM. RSGEM has been handled to the Riemann wave system and nonlinear GPE in conformable frame. Main novelty of this paper is the solutions such as complex, mixed dark–bright, and hyperbolic in conformable operator were extracted. Via graphical illustrations, the dynamical behaviors of solutions found have been reported. The stability properties of the obtained solutions have been introduced, as well. Moreover, the strain conditions of solutions for valid have been also given.

It is estimated that these dark solitons may be closely related to the gravitational dynamical potential [73]. MI analysis of the nonlinear Gross–Pitaevskii equation has been studied, as well. Its various wave simulations have been also plotted in Figure 17. From these results, it may be suggested that the RSGEM is a power tool to solve such nonlinear partial models arising in applied and engineering sciences. Therefore, it may be also applied to investigate deeper properties of some real-world problems [74–77].

As the future direction of this topic, it is envisaged and suggested that some important analytical schemes will be developed by the experts studying in these areas of nonlinear sciences to solve more complex PDEs. This comes from the properties of real-world problems.

Data Availability

The data that support the findings of this study are available within the article.

Conflicts of Interest

The authors declare that they have no known conflicts of interest.

Authors' Contributions

W. Gao majorly contributed and H.M. Baskonus contributed on typing collection and formal analyzing.

References

[1] S. B. Yamgoué, G. R. Deffo, and F. B. Pelap, "A new rational sine-Gordon expansion methodand its application to nonlinear wave equations arising in mathematical physics," *The European Physical Journal Plus*, vol. 134, Article ID 380, 2019.

[2] Z. Zhao and L. He, "Multiple lump solutions of the (3 + 1)-dimensional potential Yu–Toda–Sasa–Fukuyama equation," *Applied Mathematics Letters*, vol. 95, pp. 114–121, 2019.

[3] Z.-W. Xu, G.-F. Yu, and Z.-N. Zhu, "Bright–dark soliton solutions of the multi-component AB system," *Wave Motion*, vol. 83, pp. 134–147, 2018.

[4] K. U.-H. Tariq and A. R. Seadawy, "Bistable bright–dark solitary wave solutions of the (3 + 1)-dimensional breaking soliton, Boussinesq equation with dual dispersion and modified Korteweg–de Vries–Kadomtsev–Petviashvili equations and their applications," *Results in Physics*, vol. 7, pp. 1143–1149, 2017.

[5] Y. Cao, J. He, and D. Mihalache, "Families of exact solutions of a new extended (2 + 1)-dimensional Boussinesq equation," *Nonlinear Dynamics*, vol. 91, no. 4, pp. 2593–2605, 2018.

[6] S. Chen and Y. Ren, "Small amplitude periodic solution of Hopf Bifurcation Theorem for fractional differential equations of balance point in group competitive martial arts," *Applied Mathematics and Nonlinear Sciences*, vol. 7, no. 1, pp. 207–214, 2022.

[7] S. T. Abdulazeez and M. Modanli, "Analytic solution of fractional order pseudo-hyperbolic telegraph equation using

modified double laplace transform method," *International Journal of Mathematics and Computer in Engineering*, vol. 1, no. 1, pp. 105–114, 2023.

[8] A. Yokuş, "Construction of different types of traveling wave solutions of the relativistic wave equation associated with the Schrödinger equation," *Mathematical Modelling and Numerical Simulation with Applications*, vol. 1, no. 1, pp. 24–31, 2021.

[9] A.-M. Wazwaz, "Bright and dark optical solitons for $(2+1)$-dimensional Schrödinger (NLS) equations in the anomalous dispersion regimes and the normal dispersive regimes," *Optik*, vol. 192, Article ID 162948, 2019.

[10] A.-M. Wazwaz, "Multiple complex and multiple real soliton solutions for the integrable sine–Gordon equation," *Optik*, vol. 172, pp. 622–627, 2018.

[11] H. F. Ismael, H. M. Baskonus, H. Bulut, and W. Gao, "Instability modulation and novel optical soliton solutions to the Gerdjikov–Ivanov equation with M-fractional," *Optical and Quantum Electronics*, vol. 55, pp. 1–15, Article ID 303, 2023.

[12] C. C. Hu, Y. S. Deng, B. Tian, Y. Sun, and C. R. Zhang, "Rational and semi-rational solutions for the $(3+1)$-dimensional B-type Kadomtsev Petviashvili Boussinesq equation," *Modern Physics Letters B*, vol. 1950296, pp. 1–10, 2019.

[13] N. A. Kudryashov, "Traveling wave reduction of the modified KdV hierarchy: the lax pair and the first integrals," *Communications in Nonlinear Science and Numerical Simulation*, vol. 73, pp. 472–480, 2019.

[14] B. Ghanbari, M. S. Osman, and D. Baleanu, "Generalized exponential rational function method for extended Zakharov–Kuzetsov equation with conformable derivative," *Modern Physics Letters A*, vol. 34, no. 20, Article ID 1950155, 2019.

[15] Y. Yao, G. Ma, X. Zhang, and W. Liu, "M-typed dark soliton generation in optical fibers," *Optik*, vol. 193, Article ID 162997, 2019.

[16] D. Arslan, "The comparison study of hybrid method with RDTM for solving Rosenau–Hyman equation," *Applied Mathematics and Nonlinear Sciences*, vol. 5, no. 1, pp. 267–274, 2020.

[17] Ö. Özer, "A handy technique for fundamental unit in specific type of real quadratic fields," *Applied Mathematics and Nonlinear Sciences*, vol. 5, no. 1, pp. 495–498, 2020.

[18] F. Dusunceli, "New exact solutions for generalized $(3+1)$ shallow water-like (SWL) equation," *Applied Mathematics and Nonlinear Sciences*, vol. 4, no. 2, pp. 365–370, 2019.

[19] M. A. Akbar, F. Mahmud, A.-M. Wazwaz et al., "Dynamical behavior of solitons of the perturbed nonlinear Schrödinger equation and microtubules through the generalized Kudryashov scheme," *Results in Physics*, vol. 43, Article ID 106079, 2022.

[20] M. S. Osman, K. U. Tariq, A. Bekir et al., "Investigation of soliton solutions with different wave structures to the $(2+1)$-dimensional Heisenberg ferromagnetic spin chain equation," *Communications in Theoretical Physics*, vol. 72, no. 3, Article ID 035002, 2020.

[21] C. Park, R. I. Nuruddeen, K. K. Ali, L. Muhammad, M. S. Osman, and D. Baleanu, "Novel hyperbolic and exponential ansatz methods to the fractional fifth-order Korteweg–de Vries equations," *Advances in Difference Equations*, vol. 2020, no. 1, Article ID 627, 2020.

[22] K. S. Nisar, O. A. Ilhan, S. T. Abdulazeez, J. Manafian, S. A. Mohammed, and M. S. Osman, "Novel multiple soliton solutions for some nonlinear PDEs via multiple exp-function method," *Results in Physics*, vol. 21, Article ID 103769, 2021.

[23] K. K. Ali, M. A. Abd El Salam, E. M. H. Mohamed, B. Samet, S. Kumar, and M. S. Osman, "Numerical solution for generalized nonlinear fractional integro-differential equations with linear functional arguments using Chebyshev series," *Advances in Difference Equations*, vol. 2020, no. 1, Article ID 494, 2020.

[24] I. Siddique, M. M. M. Jaradat, A. Zafar, K. Bukht Mehdi, and M. S. Osman, "Exact traveling wave solutions for two prolific conformable M-fractional differential equations via three diverse approaches," *Results in Physics*, vol. 28, Article ID 104557, 2021.

[25] Y. Saliou, S. Abbagari, A. Houwe et al., "W-shape bright and several other solutions to the $(3+1)$-dimensional nonlinear evolution equations," *Modern Physics Letters B*, vol. 35, no. 30, Article ID 2150468, 2021.

[26] S. M. Yiasir Arafat, K. Fatema, S. M. Rayhanul Islam, M. E. Islam, M. Ali Akbar, and M. S. Osman, "The mathematical and wave profile analysis of the Maccari system in nonlinear physical phenomena," *Optical and Quantum Electronics*, vol. 55, no. 2, Article ID 136, 2023.

[27] M. A. Akbar, F. A. Abdullah, M. T. Islam, M. A. A. Sharif, and M. S. Osman, "New solutions of the soliton type of shallow water waves and superconductivity models," *Results in Physics*, vol. 44, Article ID 106180, 2023.

[28] M. S. Osman, H. Rezazadeh, M. Eslami, A. Neirameh, and M. Mirzazadeh, "Analytical study of solitons to Benjamin–Bona–Mahony–Peregrine equation with power law nonlinearity by using three methods," *UPB Scientific Bulletin, Series A: Applied Mathematics and Physics*, vol. 80, no. 4, pp. 267–278, 2018.

[29] Q. Zhao, J. Liu, H. Yang, H. Liu, G. Zeng, and B. Huang, "High birefringence d-shaped germanium-doped photonic crystal fiber sensor," *Micromachines*, vol. 13, no. 6, Article ID 826, 2022.

[30] W. Xu, S. Qu, and C. Zhang, "Fast terminal sliding mode current control with adaptive extended state disturbance observer for PMSM system," *IEEE Journal of Emerging and Selected Topics in Power Electronics*, vol. 11, no. 1, pp. 418–431, 2023.

[31] L. Sun, J. Hou, C. Xing, and Z. Fang, "A robust Hammerstein–Wiener model identification method for highly nonlinear systems," *Processes*, vol. 10, no. 12, Article ID 2664, 2022.

[32] S. Liu and C. Liu, "Virtual-vector-based robust predictive current control for dual three-phase PMSM," *IEEE Transactions on Industrial Electronics*, vol. 68, no. 3, pp. 2048–2058, 2021.

[33] J. Liu, S. MAO, S. Song, L. Huang, L. A. Belfiore, and J. Tang, "Towards applicable photoacoustic micro-fluidic pumps: tunable excitation wavelength and improved stability by fabrication of Ag–Au alloying nanoparticles," *Journal of Alloys and Compounds*, vol. 884, Article ID 161091, 2021.

[34] Z. Shao, Q. Zhai, Z. Han, and X. Guan, "A linear AC unit commitment formulation: an application of data-driven linear power flow model," *International Journal of Electrical Power & Energy Systems*, vol. 145, Article ID 108673, 2023.

[35] F. Bouchaala, M. Y. Ali, J. Matsushima et al., "Estimation of seismic wave attenuation from 3d seismic data: a case study of

OBC data acquired in an offshore oilfield," *Energies*, vol. 15, no. 2, Article ID 534, 2022.

[36] F. Bouchaala, M. Y. Ali, and J. Matsushima, "Compressional and shear wave attenuations from walkway VSP and sonic data in an offshore Abu Dhabi oilfield," *Comptes Rendus. Géoscience*, vol. 353, no. 1, pp. 337–354, 2021.

[37] J. Matsushima, M. Y. Ali, and F. Bouchaala, "Propagation of waves with a wide range of frequencies in digital core samples and dynamic strain anomaly detection: carbonate rock as a case study," *Geophysical Journal International*, vol. 224, no. 1, pp. 340–354, 2021.

[38] F. Bouchaala, M. Y. Ali, J. Matsushima et al., "Azimuthal investigation of compressional seismic-wave attenuation in a fractured reservoir," *GEOPHYSICS*, vol. 84, no. 6, pp. B437–B446, 2019.

[39] S. Srinivasareddy, Y. V. Narayana, and D. Krishna, "Sector beam synthesis in linear antenna arrays using social group optimization algorithm," *National Journal of Antennas And Propagation*, vol. 3, no. 2, pp. 6–9, 2021.

[40] S. Liu and C. Liu, "Direct harmonic current control scheme for dual three-phase PMSM drive system," *IEEE Transactions on Power Electronics*, vol. 36, no. 10, pp. 11647–11657, 2021.

[41] S. Liu, C. Liu, H. Zhao, Y. Liu, and Z. Dong, "Improved flux weakening control strategy for five-phase PMSM considering harmonic voltage vectors," *IEEE Transactions on Power Electronics*, vol. 37, no. 9, pp. 10967–10980, 2022.

[42] F. Liu, T. Zhang, D. M. Alghazzawi, and M. A. A. Soltan, "Optimisation of modelling of finite element differential equations with modern art design theory," *Applied Mathematics and Nonlinear Sciences*, vol. 7, no. 2, pp. 277–284, 2022.

[43] M. Bilal, H. Haris, A. Waheed, and M. Faheem, "The analysis of exact solitons solutions in monomode optical fibers to the generalizednonlinear Schrödinger system by the compatible techniques," *International Journal of Mathematics and Computer in Engineering*, vol. 1, no. 2, pp. 149–170, 2023.

[44] V. C. Johnson, J. S. Bali, C. B. Kolanur, and S. Tanwashi, "Industry 4.0: intelligent quality control and surface defect detection," *3C Empresa. Investigación y Pensamiento Crítico*, vol. 11, no. 2, pp. 186–192, 2022.

[45] S. A. Choudhari, M. A. Kumbhalkar, D. V. Bhise, and M. M. Sardeshmukh, "Optimal reservoir operation policy determination for uncertainty conditions," *3C Empresa. Investigación y Pensamiento Crítico*, vol. 11, no. 2, pp. 277–295, 2022.

[46] J. Lu, L. Zhu, and W. Gao, "Remarks on bipolar cubic fuzzy graphs and its chemical applications," *International Journal of Mathematics and Computer in Engineering*, vol. 1, no. 1, pp. 1–10, 2023.

[47] B. Xu, Y. Zhang, and S. Zhang, "Line soliton interactions for shallow ocean-waves and novel solutions with peakon, ring, conical, columnar and lump structures based on fractional KP equation," *Advances in Mathematical Physics*, vol. 2021, Article ID 6664039, 15 pages, 2021.

[48] B. Xu, Y. Zhang, and S. Zhang, "Fractional rogue waves with translational coordination, steep crest and modified asymmetry," *Complexity*, vol. 2021, Article ID 6669087, 14 pages, 2021.

[49] Y. Gu, B. Chen, F. Ye, and N. Aminakbari, "Soliton solutions of nonlinear Schrödinger equation with the variable coefficients under the influence of Woods–Saxon potential," *Results in Physics*, vol. 42, Article ID 105979, 2022.

[50] Y. Gu and L. Liao, "Closed form solutions of Gerdjikov–Ivanov equation in nonlinear fiber optics involving the beta derivatives," *International Journal of Modern Physics B*, vol. 36, no. 19, Article ID 2250116, 2022.

[51] Y. Gu, W. Yuan, N. Aminakbari, and J. Lin, "Meromorphic solutions of some algebraic differential equations related Painlevé equation IV and its applications," *Mathematical Methods in the Applied Sciences*, vol. 41, no. 10, pp. 3832–3840, 2018.

[52] Y. Wang, P. Veeresha, D. G. Prakasha, H. Mehmet Baskonus, and W. Gao, "Regarding deeper properties of the fractional order Kundu–Eckhaus equation and massive thirring model," *Computer Modeling in Engineering & Sciences*, vol. 133, no. 3, pp. 697–717, 2022.

[53] Y. Gu and N. Aminakbari, "Bernoulli (G'/G) -expansion method for nonlinear Schrödinger equation with third-order dispersion," *Modern Physics Letters B*, vol. 36, no. 11, Article ID 2250028, 2022.

[54] L. Yan, Z. Sabir, E. Ilhan, M. Asif Zahoor Raja, W. Gao, and H. Mehmet Baskonus, "Design of a computational heuristic to solve the nonlinear liénard differential model," *Computer Modeling in Engineering & Sciences*, vol. 136, no. 1, pp. 201–221, 2023.

[55] S. Raut, S. Saha, A. N. Das, and P. Talukder, "Complete discrimination system method for finding exact solutions, dynamical properties of combined Zakharsov–Kuznetsov-modified Zakarsov–Kuznetsov equation," *Alexandria Engineering Journal*, vol. 76, pp. 247–257, 2023.

[56] Y. Gu and W. Yuan, "Closed form solutions of nonlinear space-time fractional Drinfel'd–Sokolov–Wilson equation via reliable methods," *Mathematical Methods in the Applied Sciences*, pp. 1–17, 2021.

[57] M. Inc, E. A. Az-Zo'bi, A. Jhangeer, H. Rezazadeh, M. Nasir Ali, and M. K. A. Kaabar, "New soliton solutions for the higher-dimensional non-local ito equation," *Nonlinear Engineering*, vol. 10, no. 1, pp. 374–384, 2021.

[58] E. Az-Zo'bi, L. Akinyemi, and A. O. Alleddawi, "Construction of optical solitons for conformable generalized model in nonlinear media," *Modern Physics Letters B*, vol. 35, no. 24, Article ID 2150409, 2021.

[59] Z. Altawallbeh, E. Az-Zo'bi, A. O. Alleddawi, M. Şenol, and L. Akinyemi, "Novel liquid crystals model and its nematicons," *Optical and Quantum Electronics*, vol. 54, no. 12, Article ID 861, 2022.

[60] R. Ur Rahman, W. A. Faridi, M. A. El-Rahman, A. Taishiyeva, R. Myrzakulov, and E. A. Az-Zo'bi, "The sensitive visualization and generalized fractiona solitons' construction fo regularized long-wave governing model," *Fractal and Fractional*, vol. 7, no. 2, Article ID 136, 2023.

[61] R. U. Rahman, A. F. Al-Maaitah, M. Qousini, E. A. Az-Zo'bi, S. M. Eldin, and M. Abuzar, "New soliton solutions and modulation instability analysis of fractional Huxley equation," *Results in Physics*, vol. 44, Article ID 106163, 2023.

[62] H. K. Barman, A. R. Seadawy, M. A. Akbar, and D. Baleanu, "Competent closed form soliton solutions to the Riemann wave equation and the Novikov–Veselov equation," *Results in Physics*, vol. 17, Article ID 103131, 2020.

[63] P. R. Kundu, M. R. A. Fahim, M. E. Islam, and M. A. Akbar, "The sine-Gordon expansion method for higher-dimensional NLEEs and parametric analysis," *Heliyon*, vol. 7, no. 3, Article ID e06459, 2021.

[64] A. V. Gurevich, A. L. Krylov, and G. A. El, "Evolution of a Riemann wave in dispersive hydrodynamics," *Soviet Physics - JETP*, vol. 74, no. 6, pp. 957–962, 1992.

[65] Q.-Y. Li, Z.-D. Li, L. Li, and G.-S. Fu, "Nonautonomous bright and dark solitons of Bose–Einstein condensates with feshbach-managed time-dependent scattering length," *Optics Communications*, vol. 283, no. 17, pp. 3361–3366, 2010.

[66] Z. X. Liang, Z. D. Zhang, and W. M. Liu, "Dynamics of a bright soliton in Bose–Einstein condensates with time-dependent atomic scattering length in an expulsive parabolic potential," *Physical Review Letters*, vol. 94, no. 5, Article ID 050402, 2005.

[67] V. M. Pérez-García, V. V. Konotop, and V. A. Brazhnyi, "Feshbach resonance induced shock waves in Bose–Einstein condensates," *Physical Review Letters*, vol. 92, no. 22, Article ID 220403, 2004.

[68] W. Gao, G. Yel, H. M. Baskonus, and C. Cattani, "Complex solitons in the conformable $(2+1)$-dimensional Ablowitz–Kaup–Newell–Segur equation," *AIMS Mathematics*, vol. 5, no. 1, pp. 507–521, 2020.

[69] A. Kumar, E. Ilhan, A. Ciancio, G. Yel, and H. M. Baskonus, "Extractions of some new travelling wave solutions to the conformable DateJimbo–Kashiwara–Miwa equation," *AIMS Mathematics*, vol. 6, no. 5, pp. 4238–4264, 2021.

[70] J. L. G. Guirao, H. M. Baskonus, and A. Kumar, "Regarding new wave patterns of the newly extended nonlinear $(2+1)$-dimensional Boussinesq equation with fourth order," *Mathematics*, vol. 8, no. 3, Article ID 341, 2020.

[71] S. Chandrasekhar, *Hydrodynamic and Hydromagnetic Stability*, Dover Publications Inc., New York, United States, 1981.

[72] B. Sandstede, "Chapter 18: stability of travelling waves," *Handbook of Dynamical Systems*, vol. 2, pp. 983–1055, 2002.

[73] E. W. Weisstein, *Concise Encyclopedia of Mathematics*, CRC, New York, 2nd edition, 2002.

[74] J. Pan, M. U. Rahman, and Rafiullah, "Breather-like, singular, periodic, interaction of singular and periodic solitons, and a-periodic solitons of third-order nonlinear Schrödinger equation with an efficient algorithm," *The European Physical Journal Plus*, vol. 138, Article ID 912, 2023.

[75] J. Manafian and M. Lakestani, "N-lump and interaction solutions of localized waves to the (2+1)-dimensional variable-coefficient Caudrey–Dodd–Gibbon–Kotera–Sawada equation," *Journal of Geometry and Physics*, vol. 150, Article ID 103598, 2020.

[76] T. Mathanaranjan, "Optical solitons and stability analysis for the new $(3+1)$-dimensional nonlinear Schrödinger equation," *Journal of Nonlinear Optical Physics & Materials*, vol. 32, no. 2, Article ID 2350016, 2023.

[77] S. Kumar and M. Niwas, "Exploring lump soliton solutions and wave interactions using new inverse G'/G-expansion approach: applications to the $(2+1)$-dimensional nonlinear Heisenberg ferromagnetic spin chain equation," *Nonlinear Dynamics*, vol. 111, pp. 20257–20273, 2023.